Dilute nitride GaInNAs and GaInNAsSb solar cells by molecular beam epitaxy

David B. Jackrel,[a] Seth R. Bank, Homan B. Yuen, Mark A. Wistey, and James S. Harris, Jr.
Solid State Electronics Laboratory, Stanford University, Stanford, California 94305

Aaron J. Ptak, Steven W. Johnston, Daniel J. Friedman, and Sarah R. Kurtz
National Renewable Energy Laboratory, Golden, Colorado 80401

(Received 10 January 2007; accepted 18 April 2007; published online 14 June 2007)

Dilute nitride films with a roughly 1 eV band gap can be lattice-matched to gallium arsenide and germanium, and therefore could become a critical component in next-generation multijunction solar cells. To date most dilute nitride solar cells have been plagued with poor efficiency, due in large part to short diffusion lengths. This study focuses on two techniques aimed at improving the quality of dilute nitride films grown by molecular beam epitaxy: the utilization of biased deflection plates installed in front of the nitrogen plasma source, and the introduction of antimony during growth. Results from GaInNAs cells grown with and without deflection plates, and GaInNAsSb solar cells are reported. The use of biased deflection plates during GaInNAs growth improved every aspect of solar cell performance. For the GaInNAs devices grown with deflection plates, the dark current density, open-circuit voltage, and fill factor were the best of the devices studied. The GaInNAsSb cells had the highest quantum efficiency, almost 80% at maximum, mainly due to low background doping densities providing these devices with wide depletion widths. The GaInNAsSb materials also had quite narrow band gaps of 0.92 eV. Because of the high collection efficiency coupled with the narrow band gap, the sub-GaAs short-circuit current density produced by the GaInNAsSb cells is 14.8 mA/cm^2, which was the highest of the devices studied. This current is nearly 50% greater than the best dilute nitride solar cells in the literature, and is the first dilute nitride cell to produce enough current to current match the upper two subcells in a triple-junction device, composed of GaInP/InGaAs/GaInNAsSb. © *2007 American Institute of Physics*. [DOI: 10.1063/1.2744490]

I. INTRODUCTION AND BACKGROUND

The current world record efficiency solar cell is a triple-junction cell, composed of GaInP/InGaAs/Ge, with an efficiency of 39.3% measured at 179 suns concentration.[1] This world record device is metamorphic, but the best lattice-matched GaInP/InGaAs/Ge solar cell has an efficiency that is very similar: 39.0% at 236 suns concentration.[2] The InGaAs middle junction of the lattice-matched cell has a band gap of 1.4 eV. However, monolithic multijunction cell efficiencies could benefit from materials with band gaps between 0.95 and 1.3 eV (depending on the use of three or four junctions and the concentration ratio).[3] This explains the slightly higher efficiencies possible using metamorphic structures. The dilute nitrides, GaInNAs and GaInNAsSb, are two of the only known material systems that have band gaps between 0.9 and 1.3 eV while remaining lattice-matched to germanium. These materials can raise device efficiency without the need for metamorphic structures, which inherently contain many defects in the graded region, are generally thicker due to the graded buffer layer, and are more difficult to manufacture than lattice-matched structures. It is also possible to create triple-junction cells using a dilute nitride subcell instead of a germanium subcell, such as a lattice-matched GaInP/GaAs/GaInNAs(Sb) cell, where the GaInNAs(Sb) subcell has a band gap near 0.9 eV. Such a cell has an ideal efficiency of 44.5% under the 500-sun low-AOD (aerosol optical depth) solar spectrum, which is higher than the ideal efficiency of the current GaInP/GaAs/Ge cells, 40%.[4] The elimination of the thick germanium subcell also enables other applications, such as very light or flexible solar cells, and cogeneration using the photons with energy below 0.9 eV.

Recently, GaInNAs solar cells were created with nearly 100% quantum efficiency, but they all had band gaps larger than 1.15 eV.[5] Narrow band gap GaInNAs solar cells with band gaps at or below 1.0 eV are plagued with poor performance due to short diffusion lengths coupled with narrow depletion widths.[6] This can be related to the increased nitrogen content required to achieve the lower band gap materials. A narrow band gap dilute nitride cell with high efficiency makes possible various multijunction structures, such as those mentioned above.

In highly strained GaInNAs films, such as quantum wells used in laser structures, the material quality and laser performance can be greatly improved through the introduction of antimony during molecular beam epitaxy (MBE) growth.[7–10] The exact role of antimony during dilute nitride growth is not conclusively known. It has been proposed that antimony acts as a reactive surfactant, with the antimony atoms segregating to the growth surface and incorporating into the film in only dilute concentrations.[10] The incorpora-

[a]Electronic mail: djackrel@stanfordalumni.org

 © 2007 American Institute of Physics

Downloaded 13 Jul 2007 to 171.66.249.62. Redistribution subject to AIP license or copyright, see http://jap.aip.org/jap/copyright.jsp

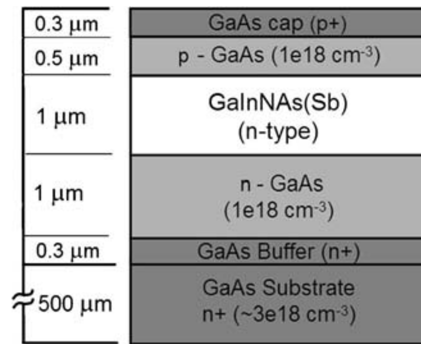

FIG. 1. Schematic of MBE-grown GaInNAs(Sb) devices.

tion of antimony decreases the band gap in dilute nitride films, and increases the lattice constant rather than decreasing it as nitrogen does.[7–10] Antimony is also known to increase the nitrogen incorporation in dilute nitrides, which further lowers the band gap, and also has the effect of offsetting the larger lattice constants caused by the incorporation of antimony.[9–11]

Biased deflection plates installed in front of the rf-plasma nitrogen sources used to produce active nitrogen in MBE have been used to improve the material quality in thin, highly strained GaInNAs films as well. A moderate dc bias (−40 V) applied across the plates creates an electric field which deflects the high-energy charged species in the plasma away from the growing film surface.[10,12] Strained GaInNAs quantum wells have been grown using deflection plates that displayed higher photoluminescence intensity than similar films grown without deflection plate bias, which indicates a reduction in the nonradiative recombination associated with ion damage induced point defects.[8,9] The lasers produced from these quantum well structures also displayed lower threshold currents and higher lasing efficiencies.

This study focuses on two techniques aimed at improving the quality of thicker narrow band gap, nearly lattice-matched dilute nitride films and solar cells grown by MBE: the utilization of biased deflection plates installed in front of the nitrogen plasma source, and the introduction of antimony to the growth process.

II. EXPERIMENTAL DETAILS

GaInNAs and GaInNAsSb double-heterostructure PIN diodes were grown at the Solid State Electronics Laboratory at Stanford University on (100) GaAs substrates using a load-locked Varian model Gen II solid-source MBE machine with nitrogen supplied by an SVT Associates model 4.5 rf-plasma cell. One GaInNAs structure was grown without the use of deflection plates (hereafter referred to as "GaInNAs"), one GaInNAs structure was grown using deflection plates [hereafter referred to as "GaInNAs (DP)"], and a third structure incorporated a GaInNAsSb active layer, and was also grown using biased deflection plates (hereafter referred to as "GaInNAsSb"). The system and growth details have been reported previously.[7] For the samples grown using the deflection plate bias, one plate was maintained at −40 V and one maintained at ground. A schematic of the growth structure is illustrated in Fig. 1. The active layer of each sample was unintentionally doped. The active GaInNAs(Sb) material is 1 μm thick, composed of approximately 1–2% N and approximately 5–7% In (and approximately 2–6% Sb for the Sb-containing sample). These compositions gave material that was close to lattice-matched to GaAs (the lattice constants and degree of relaxation will be discussed in a later section). The wider band gap n and p barrier layers of the double heterostructures are GaAs with dopant densities equal to roughly 10^{18} cm^{-3}. After growth, annealing was performed on the dilute nitride materials in a similar manner as that required to achieve low-threshold current lasers, using a rapid thermal anneal with arsenic out-diffusion limited by a GaAs proximity cap.[7] The postgrowth annealing temperature of the dilute nitride materials is experimentally optimized for each sample by maximizing the peak photoluminescence (PL) intensity.

Solar cell devices were fabricated from these samples at the National Renewable Energy Laboratory (NREL). The front contacts are Au and the back contacts are annealed Au/Sn/Au. Internal quantum efficiency spectra are determined by dividing the external quantum efficiency by $(1-R)$, where R is the measured specular reflectivity. Light current-voltage photovoltaic measurements were performed using AM1.5 low-AOD solar conditions. The light intensity was adjusted to simulate the photocurrent density under a GaAs subcell in a monolithic multijunction device, as determined by the device quantum efficiency and the AM1.5 low-AOD solar spectrum.[13] A GaAs filter was placed over the samples during *L-I-V* experiments to approximate the correct spectral content for the lower subcell in a monolithic multijunction device.

Fourier transform deep-level transient spectroscopy (DLTS) was performed using a FT-DLTS system with a cryostat temperature range from 30 to 400 K. Threading dislocation density measurements were performed using spectral cathodoluminescence (CL) imaging using a Roper Scientific OMA V InGaAs 512×1 photodiode array, and a Acton SpectraPro-500i spectrograph.[14,15] Time-resolved PL measurements were performed using a 1060 nm wavelength titanium:sapphire laser source with a 250 kHz repetition rate and a pulse width of several tenths of picoseconds, a Spex 320M spectrometer, and a Hamamatsu R5509 red-sensitive photomultiplier tube cooled to 80 K. X-ray diffraction (XRD) measurements were performed using a Phillips X'Pert PRO diffractometer, equipped with triple-axis incident optics for high-resolution scans.

III. DEVICE RESULTS

A. Spectral quantum efficiency

Figure 2 plots the internal quantum efficiency (IQE) of representative devices from the GaInNAs, GaInNAs (DP), and GaInNAsSb solar cells produced. The absorption edges of the materials closely correspond to the band gaps as measured by PL: GaInNAs, 1.08 eV; GaInNAs (DP), 1.03 eV; and GaInNAsSb, 0.92 eV. The use of deflection plates has increased the IQE of the GaInNAs cell from 56% to 68% at maximum. The addition of antimony drives the device IQE even higher, reaching 79% at maximum. The GaInNAsSb

Downloaded 13 Jul 2007 to 171.66.249.62. Redistribution subject to AIP license or copyright, see http://jap.aip.org/jap/copyright.jsp

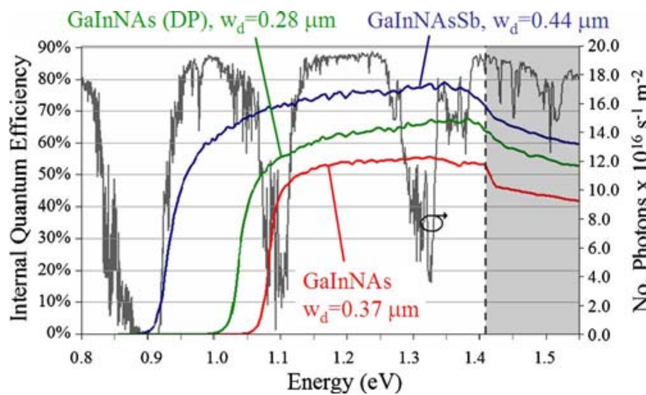

FIG. 2. (Color online) GaInNAs, GaInNAs (DP), and GaInNAsSb internal quantum efficiency spectra and AM1.5 low-AOD solar spectrum. The dotted line is at 1.42 eV, the band gap of the GaAs, which is the point at which the upper layers of the PIN devices (or the subcell above in a multijunction stack) begin to absorb. The short-circuit depletion widths are also noted for each device.

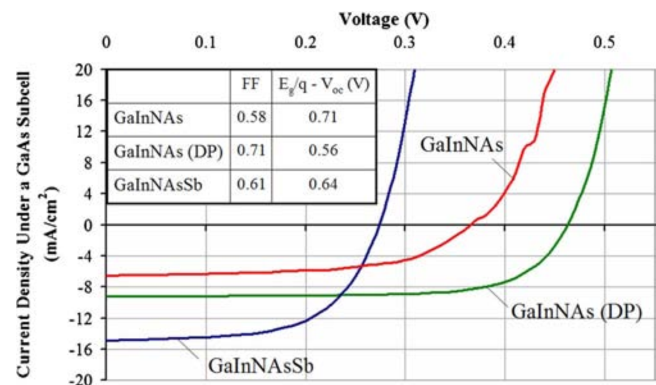

FIG. 3. (Color online) Photocurrent-voltage characteristics of dilute nitride solar cells with the light intensity and spectral content adjusted to simulate conditions underneath a GaAs subcell in a multijunction stack.

device represents one of the smallest band gaps achieved (0.92 eV) in a dilute nitride solar cell with high carrier collection efficiency.[5,16–18] Table I compares the properties of various dilute nitride devices from the literature with devices from this study, including the short-circuit current density that would be produced beneath a GaAs subcell in a monolithic multijunction stack.

The GaInNAsSb subcell would produce a short-circuit current density of 14.8 mA/cm^2, underneath a GaAs subcell in a multijunction structure, as determined using the IQE and the low-AOD spectrum truncated at 880 nm to simulate the light-filtering effect of the overlying GaAs subcell.[13] Under the same conditions, the GaInNAs (DP) devices have a short-circuit current density of 9.0 mA/cm^2. Reflection losses were not included in the calculation, although these losses are expected to be less than a few percent with a high-quality antireflection coating. The larger photocurrent in the GaInNAsSb devices reflects both the increased photoresponse as well as the lower band gap. The current world record triple-junction device composed of lattice-matched GaInP/InGaAs/Ge has a short-circuit current density of 3.377 A/cm^2 at 236 suns, or 14.3 mA/cm^2 at 1 sun.[2] This indicates that the narrow band gap GaInNAsSb cells have enough photoresponse to current match the upper two subcells in state-of-the-art triple-junction solar cells.

TABLE I. Band gap, internal quantum efficiency (at 0.2 eV above the band gap), and short-circuit current found by integrating the spectral response of the devices and the low-AOD spectrum to 880 nm (Ref. 13), thereby simulating conditions underneath a GaAs subcell in a monolithic multijunction device.

Sample	Reference	Band gap (eV)	IQE (atE_g+0.2 eV)	J_{sc} (mA/cm^2)
"GaInNAsSb"	This work	0.92	0.72	14.8
"GaInNAs (DP)"	This work	1.03	0.64	9.03
"GaInNAs"	This work	1.08	0.54	6.73
GaInNAs	17	1.04	0.74	9.64
GaInNAs	5	1.15	0.96	9.38
GaInNAs	16	1.07	0.78	9.26
GaInNAs	18	1.0	0.55	8.95
GaInNAs	18	1.1	0.67	7.79

The short-circuit depletion widths of each device, as determined from capacitance-voltage measurements, are labeled in Fig. 2 as well. The short-circuit depletion widths for the GaInNAs (DP), GaInNAs, and GaInNAsSb samples are 0.28, 0.37, and 0.44 μm, respectively. The GaInNAsSb device has the widest depletion width, which explains the high collection efficiency. The GaInNAs (DP) device has a narrower depletion width than the GaInNAs device, and yet has higher collection efficiency. This is indicative of improved materials quality achieved using deflection plates, which yield long diffusion lengths enhancing carrier collection. In a later section the relation between depletion width and background carrier concentration is discussed.

The device quantum efficiency spectra in Fig. 2 are also overlaid on the AM1.5 low-AOD solar spectrum. It is evident from this graph that the lower photocurrents of the GaInNAs and GaInNAs (DP) devices are partially the result of the lower fraction of solar irradiation available for absorption. The GaInNAs and GaInNAs (DP) devices absorb only a small fraction of the lobe of the solar spectrum between 0.92 and 1.1 eV, while the band gap of the GaInNAsSb material allows that device to absorb the entire lobe. It is interesting to note that there is a strong atmospheric absorption band from about 0.85 to 0.92 eV. Due to this region bereft of solar radiation, a solar cell with a 0.85 eV band gap will not have significantly larger photocurrent than one with a 0.92 eV band gap.

B. Photocurrent-voltage characteristics

The current-voltage response of the GaInNAs devices grown with and without deflection plates, and the GaInNAsSb cells, with the light intensity adjusted to simulate the photocurrent density under a GaAs subcell, are shown in Fig. 3. The improvement in solar cell performance suggests that the use of biased deflection plates in our MBE system during GaInNAs growth improved the material quality.

The GaInNAs (DP) cells displayed improved short-circuit current density, open-circuit voltage, fill factor, and band gap to open-circuit voltage difference compared to the GaInNAs

Downloaded 13 Jul 2007 to 171.66.249.62. Redistribution subject to AIP license or copyright, see http://jap.aip.org/jap/copyright.jsp

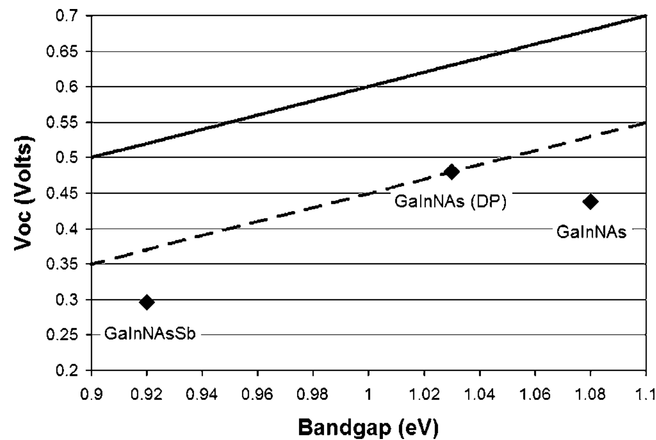

FIG. 4. Open-circuit voltage plotted vs band gap for the three devices. The solid line represents a constant band gap to open-circuit voltage difference of 0.4 eV, equivalent to what would be expected in a high-quality GaAs device. The dotted line represents a constant band gap to open-circuit voltage difference of 0.55 eV, equivalent to the value for the GaInNAs (DP) device.

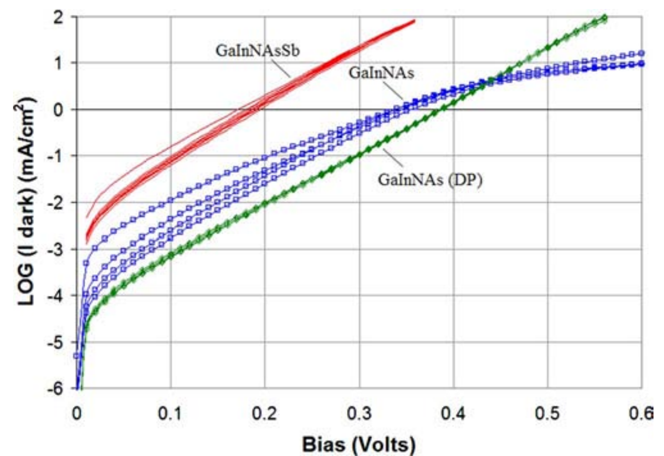

FIG. 5. (Color online) Semilog forward bias dark current-voltage characteristics of dilute nitride solar cells.

devices. However, the GaInNAs device photocurrent voltage curve has a kink just above 0.4 V, which is likely due to a parasitic junction in the device. This nonideal nature of the GaInNAs devices makes them difficult to compare with the GaInNAs (DP) and GaInNAsSb devices. The GaInNAsSb devices displayed higher short-circuit current densities than either of the GaInNAs devices; however, this device also showed the lowest open-circuit voltage, 0.28 V. A typical Ge device, however, has an open-circuit voltage of roughly 0.25 V at 1 sun.[19] Since the GaInNAsSb devices are producing sufficient current, this shows that using this material rather than Ge as the bottom junction in a triple-junction GaInP/GaAs/GaInNAsSb device does have the potential to increase the power conversion efficiency of state-of-the-art triple-junction cells by increasing the open-circuit voltage of the devices.

Figure 4 plots the open-circuit voltage of the three devices with the light intensity adjusted to give a photocurrent of $20\ \mathrm{mA/cm^2}$ in all of the devices. The solid line in the plot indicates a band gap to open-circuit voltage difference of 0.4 V, roughly the difference expected in a high-quality GaAs solar cell. All of the devices have a band gap to open-circuit voltage difference larger than 0.4 V at this photocurrent value. The most ideal device is the GaInNAs (DP) device, which has a band gap to open-circuit voltage difference of 0.55 V. The dotted line shows a constant band gap to open-circuit voltage difference of 0.55 V [equal to the GaInNAs (DP) device], and shows that the GaInNAs and GaInNAsSb band gap to open-circuit voltage differences are larger than this value. The small band gap to open-circuit voltage difference, along with the high carrier collection efficiency despite narrow depletion widths, indicates that the GaInNAs (DP) device has higher materials quality than the GaInNAsSb devices.

C. Dark current density

The dark current-voltage character can also provide insight into the materials quality and solar cell performance, and is shown for each device in a semilog scale in Fig. 5. There is a wide variation in device dark current for the four GaInNAs devices processed, but the four GaInNAs (DP) and eight GaInNAsSb devices are fairly consistent. The GaInNAs (DP) samples, grown with deflection plate bias, have the lowest dark current. The GaInNAs devices, grown without deflection plate bias, have higher dark current but the shape of the dark current voltage curves is also different. At voltages greater than the open-circuit voltage, the slope of the semilog dark current voltage curves changes. This is most likely the result of the parasitic junction present in the GaInNAs devices, and makes comparisons with the dark current of the other devices somewhat difficult. The dark current in the GaInNAsSb device, however, is the largest, and is roughly two orders of magnitude larger than the GaInNAs (DP) device. Much of the increase in dark current can be attributed to the lower band gap of the antimonide material, and is thus unavoidable. The additional increase in dark current for the GaInNAsSb devices (not accounted for by the lower band gap) could be due to a number of factors. The GaInNAsSb devices have wider depletion widths than the GaInNAs (DP) devices. Higher dark currents can be caused by increased Shockley-Read-Hall (SRH) recombination in the wider depletion regions. Higher defect concentrations, or defect species that are more effective recombination centers, could also cause increased dark current. Defect species measured by DLTS will be discussed in a later section. Furthermore, ideal diode modeling indicates that most of the decrease in fill factor in the GaInNAsSb devices is explainable by the increased dark current. The remainder of the difference in fill factor may be due to increased field-aided collection in the GaInNAsSb device.

The slope of the semilog dark current voltage curve is related to the diode ideality. It is difficult to determine the exact n-factors for the GaInNAs and GaInNAsSb devices from the dark current voltage data since series resistance has caused nonlinearity in the semilog dark current-voltage curves for these devices. However, the n-factor for the GaInNAs (DP) devices is roughly 1.4. From analysis of roughly linear regions of the GaInNAs and GaInNAsSb devices, it seems that all three devices have ideality factors

Downloaded 13 Jul 2007 to 171.66.249.62. Redistribution subject to AIP license or copyright, see http://jap.aip.org/jap/copyright.jsp

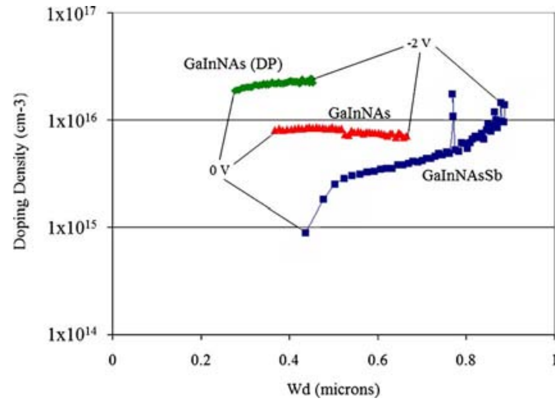

FIG. 6. (Color online) Background doping density vs depletion width.

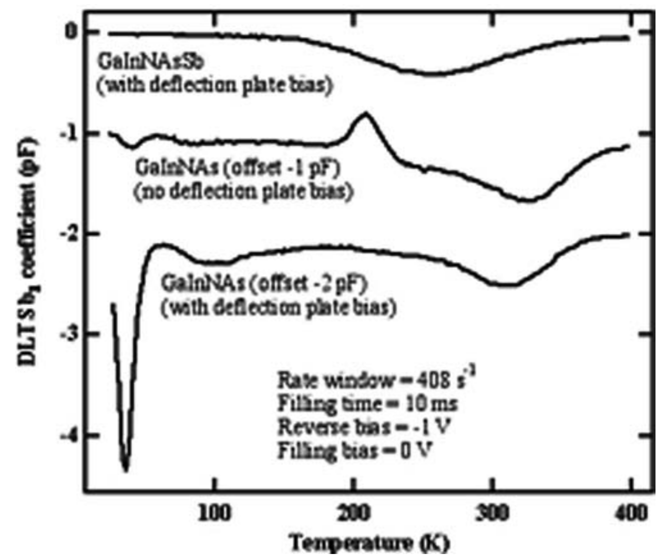

FIG. 7. Deep-level transient spectroscopy data. $b1$ Fourier coefficient of capacitance transients for all three samples. The downward-facing peaks represent electron traps and the upward-facing peaks represent hole traps.

significantly larger than 1. Due to n-factors that are greater than unity, all of the devices in this study are predicted to display a larger increase in open-circuit voltage under concentrated sunlight than would be expected from ideal diodes having $n=1$. Thus, the aforementioned advantage of the GaInNAsSb subcell over a Ge subcell in a multijunction device could be more pronounced with concentration.

IV. MATERIALS PARAMETERS

A. Background doping density

The background doping is n-type for all of the dilute nitride films in this study. The background doping densities as a function of the depletion width from capacitance-voltage measurements for representative devices of all three samples are shown in Fig. 6. The background doping density and short-circuit depletion width are inversely related for all of the samples; the lower the background doping density, the wider the short-circuit depletion width. The background doping density of the GaInNAsSb film is the lowest of the three samples, and is significantly lower than the background in the GaInNAs (DP) material. It is possible that the surfactant properties of antimony are directly responsible for the lower doping density by inhibiting the incorporation of impurities from the environment. As mentioned previously, the improved collection efficiency in the GaInNAsSb devices is due, in large part, to the wider depletion width provided by the low background doping density. The change in doping density throughout the GaInNAsSb depletion region could be caused by changes in Sb concentration. Secondary ion mass spectrometry (SIMS) data from GaInNAsSb material have shown an increase in Sb concentration toward the film surface. This would have the effect of reducing the n-type doping near the surface of the film.[20]

B. Point defect density

Figure 7 shows DLTS data for examples of the three p-i-n devices, as well as the rate window, filling time, reverse bias, and filling bias conditions. This figure shows just one Fourier component of the capacitance transients measured, but does show that there are two electron traps and one hole trap in the GaInNAs material, three electron traps in the GaInNAs (DP) material, and one electron trap in the GaInNAsSb material. All of the Fourier components were used to create Arrhenius plots to determine the trap energies, capture cross sections, and densities for each of the traps observed in the three materials. Table II summarizes these

TABLE II. Deep-level transient spectroscopy data, including trap activation energy, trap capture cross section, and trap density. "E" is used to denote electron traps, and "H" to denote hole traps. The hole trap data are taken using filling pulse times of 10 and 100 ms. The background doping density used to calculate the trap parameters for each sample is also given.

	Background doping density (cm^{-3})	Activation energy (eV)	Capture cross section (cm^2)	Trap density (cm^{-3})
GaInNAs	1.0×10^{16}			
$E1$		0.05	1.5×10^{-16}	8.3×10^{13}
$E2$		0.61	7.7×10^{-15}	2.8×10^{14}
$H1$		0.38–0.53	$1.7-4500\times10^{14}$	$1.4-2.0\times10^{14}$
GaInNAs (DP)	1.8×10^{16}			
$E1$		0.06	9.5×10^{-14}	1.8×10^{15}
$E2$		0.12	2.3×10^{-16}	1.6×10^{14}
$E3$		0.59	5.5×10^{-14}	2.4×10^{14}
GaInNAsSb	6.3×10^{15}			
$E1$		0.53	5.1×10^{-13}	1.3×10^{14}

Downloaded 13 Jul 2007 to 171.66.249.62. Redistribution subject to AIP license or copyright, see http://jap.aip.org/jap/copyright.jsp

results, as well as the background carrier concentrations in the unintentionally doped regions of these particular samples, as determined by capacitance-voltage measurements. It should be noted that, since these data were obtained from *p*-*i*-*n* structures, there is some uncertainty about which region of the device is being depleted during the measurement, and the assumption was made that all of the depletion is into the unintentionally doped (*n*-type) layer. The most important traps to consider are the traps nearest the middle of the band gap, since these traps will contribute the most strongly to SRH recombination. The GaInNAs material has two traps near the band center, one electron and one hole trap, while the GaInNAs (DP) material has only one. The GaInNAs "*E*2" electron trap and the GaInNAs (DP) "*E*3" electron trap have similar activation energy, capture cross section and density. However, the additional GaInNAs "*H*1" hole trap (whose characteristics were dependent on the time allowed to fill the minority-carrier traps) has a large capture cross section and is not present in the samples grown using deflection plate bias. On the other hand, the density of shallow electron traps is higher in the GaInNAs (DP) material than it is in the GaInNAs material. The addition of antimony has not increased the density of traps near the center of the band gap compared to the GaInNAs (DP) material, but seems to have increased the capture cross section of these traps by roughly an order of magnitude. The addition of antimony, however, has apparently eliminated the shallow electron traps.

C. Minority carrier lifetime

Time-resolved PL measurements were performed on all three structures in order to determine the minority carrier lifetime in the dilute nitride films. The minority carrier lifetime of the GaInNAs film was 0.55 ns, and the use of deflection plates improved the lifetime of the GaInNAs (DP) film to 0.74 ns. This is consistent with the improved device properties observed. The GaInNAsSb had the shortest minority carrier lifetime, 0.20 ns. This is an interesting result. Despite having the shortest carrier lifetime, the GaInNAsSb films showed the highest collection efficiency. It therefore seems likely that the increase in collection efficiency of the GaInNAsSb devices is purely a result of the increased depletion width, which in turn is a result of the low background doping density in the antimonide film.

D. Film coherence and relaxation

XRD was performed in order to determine the lattice constants of the dilute nitride films. Symmetric omega/2-theta rocking curves were done to investigate the out-of-plane (004) plane spacing, and the results are illustrated in Fig. 8. The (004) plane spacing difference between the films and GaAs substrates is about 0.5% for both the GaInNAs and GaInNAs (DP) films. The GaInNAsSb films, however, show a roughly 0.8% (004) plane spacing difference between the film and the substrate. The symmetric rocking curves give no information, however, about the in-plane lattice constants of the film, and thus reciprocal space maps of both symmetric (004) and asymmetric (224) reflections were performed to

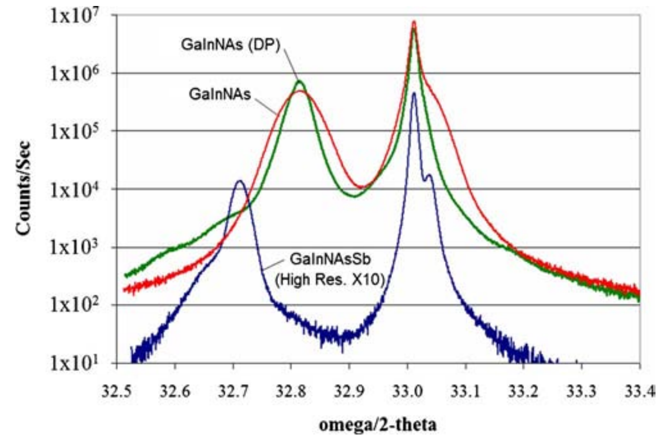

FIG. 8. (Color online) XRD omega/2-theta scans. The GaInNAsSb curve was a high-resolution scan taken with triple-axis incident optics; it was therefore a much lower intensity signal, and is shown in the figure multiplied by a factor of 10.

determine the actual degree of lattice mismatch between the film and the substrate, and to determine if the films are coherently strained or relaxed.[21]

Figures 9 and 10 show high-resolution XRD reciprocal space maps for the GaInNAs and GaInNAsSb structures, plotted versus Q_y and Q_z, in reciprocal lattice units (rlu). In Fig. 10 the vertical line labeled "coherent" denotes the case where the substrate and film peaks have the same in-plane lattice constant (although the out-of-plane lattice constant can still vary), and "relaxed" denotes a line pointing to the origin of reciprocal space, where the in-plane and out-of-plane lattice constants are equal. Figures 9 and 10 show that the GaInNAs film is virtually coherent to the substrate, but the GaInNAsSb film shows significant relaxation. From analysis of the symmetric and asymmetric reciprocal space maps, following procedures outlined by Fewster,[21] it is de-

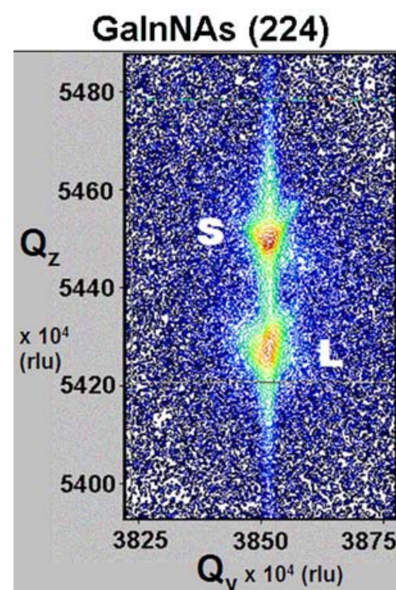

FIG. 9. (Color online) GaInNAs (224) reflection reciprocal space map. Both peaks are aligned vertically, showing the excellent coherence between the film and the substrate (S=GaAs substrate reflection, L=GaInNAs layer reflection).

Downloaded 13 Jul 2007 to 171.66.249.62. Redistribution subject to AIP license or copyright, see http://jap.aip.org/jap/copyright.jsp

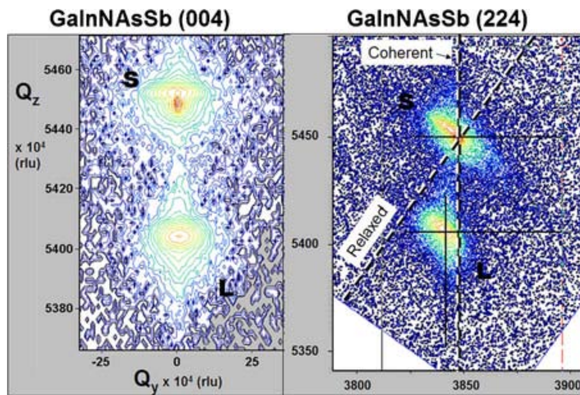

FIG. 10. (Color online) GaInNAsSb (004) reflection (left) and (224) reflection (right) reciprocal space maps (S=GaAs substrate reflection, and L=GaInNAsSb layer reflection). The center of each peak in the (224) (right) image marks the center of the reflection. The layer peak of the (224) reflection shows that the GaInNAsSb film is not completely coherent to the substrate, and has moved toward the line of relaxation.

termined that the GaInNAsSb film is about 34% relaxed, while the GaInNAs film is only about 3% relaxed. The bulk mismatch, the mismatch between the unstrained cubic lattice constant of GaInNAsSb film and the GaAs substrate, is 0.50%, while it is only 0.21% for the GaInNAs film. It is assumed that the cubic anisotropic elastic constants of the dilute nitride films are equal to those of InGaAs with similar indium compositions as in the dilute nitride films, that all stresses are biaxial, and that the tilt is zero.

It is interesting to note that the GaInNAsSb films were significantly more relaxed than either of the GaInNAs films, and yet showed the highest collection efficiency. Other device characteristics of the antimonide solar cells, however, such as open-circuit voltage, were somewhat degraded compared to the GaInNAs (DP) devices. It is possible that, if better lattice-matching between film and substrate were achieved, then some improvement in materials properties and device characteristics could result. On the other hand, the relaxation in the antimonide film does not seem to have created any additional threading dislocations, as measured by CL imaging. The threading dislocation density (TDD) in all of the structures was relatively low, and there was not much difference detected between the different structures. The GaInNAs film had a TDD of roughly 1×10^5 cm^{-2}, the GaInNAs (DP) film was $1-5\times10^5$ cm^{-2}, and the GaInNAsSb had a slightly lower TDD, below 1×10^5 cm^{-2} (which is the lower resolution limit of the technique). Finally, however, it is noted that antimony is known to vastly improve the properties of highly *strained* narrow band gap dilute nitride quantum wells in laser structures,[7–10] and it is possible that completely lattice-matched *unstrained* dilute nitride material might not show the same benefits from the incorporation of antimony.

V. CONCLUSION

Dilute nitride, GaInNAs(Sb), films were grown with and without biased deflection plates, and with and without antimony, and solar cells were fabricated from these materials. The biased deflection plates improved every aspect of GaInNAs solar cell performance. It is possible that the use of deflection plates reduced the dark current density in the GaInNAs films, which would partially explain the improvement in solar cell characteristics. However, the presence of a parasitic junction in the GaInNAs devices makes it difficult to determine all of the effects of the deflection plates with certainty. The materials grown using deflection plate bias also have no observed hole traps near the middle of the band gap. The use of antimony in the GaInNAsSb solar cells improved the collection efficiency, but degraded the open-circuit voltage and fill factor. Nevertheless, the GaInNAsSb devices are the first dilute nitride solar cells to generate enough short-circuit current to current-match to the upper subcells in a state-of-the-art three-junction solar cell. The open-circuit voltage of the GaInNAsSb solar cells was also higher than that of Ge cells at 1-sun illumination.[19] The improved collection efficiency of the antimonide devices is largely the result of wide depletion widths created by low background doping densities. The antimony-containing film showed substantially increased dark current compared to the GaInNAs (DP) devices, but much of this increase is due to the smaller band gap of the antimonide material, and is thus unavoidable. The GaInNAsSb material was also the only film studied to exhibit significant film relaxation due to a larger lattice constant mismatch between the film and the GaAs substrate. However, no increase in threading dislocation density was observed compared with the other GaInNAs structures. It is therefore difficult to determine the effects, if any, of the film relaxation, but it is possible that higher-quality material could be grown if better lattice-matching were achieved. The high collection efficiency and resulting short-circuit current density of the GaInNAsSb devices warrant further study of this material as a potential candidate for next-generation multijunction solar cells with greater than 40% efficiency.

ACKNOWLEDGMENTS

This material is based on work supported by the NSF under Grants No. 9900793 and No. 0140297. NREL's contribution to this work was completed under Contract No. DE-AC36-99GO10337 with the U.S. Department of Energy, and is subject to a government license. The authors would like to thank Manuel Romero at NREL for spectral CL imaging, and Wyatt Metzger at NREL for time-resolved PL measurements.

[1]R. R. King, R. A. Sherif, D. C. Law, J. T. Yen, M. Haddad, C. M. Fetzer, K. M. Edmondson, G. S. Kinsey, H. Yoon, M. Joshi, S. Mesropian, H. L. Cotal, D. D. Krut, J. H. Ermer, and N. H. Karam, presented at the 21st European Photovoltaic Solar Energy Conference and Exhibition, Dresden, Germany, 4–8 September (2006).
[2]R. R. King, D. C. Law, C. M. Fetzer, R. A. Sherif, K. M. Edmondson, S. Kurtz, G. S. Kinsey, H. L. Cotal, D. D. Krut, J. H. Ermer, and N. H. Karam, presented at the 20th European Photovoltaic Solar Energy Conference and Exhibition, Barcelona, Spain, 6–10 June (2005).
[3]M. A. Green, *Third Generation Photovoltaics: Advanced Solar Energy Conversion* (Springer, Berlin, 2003).
[4]D. J. Friedman, S. R. Kurtz, and J. F. Geisz, in Conference Record of the Twenty-ninth IEEE Photovoltaic Specialists Conference, New Orleans, Louisiana, 19–24 May (2002), p. 856–859.
[5]A. J. Ptak, D. J. Friedman, K. Sarah, and R. C. Reedy, J. Appl. Phys. **98**, 094501 (2005).

Downloaded 13 Jul 2007 to 171.66.249.62. Redistribution subject to AIP license or copyright, see http://jap.aip.org/jap/copyright.jsp

[6]D. J. Friedman, A. J. Ptak, S. R. Kurtz, and J. F. Geisz, in Conference Record of the Thirty-first IEEE Photovoltaic Specialists Conference, Lake Buena Vista, Florida, 3–7 January (2005), p. 691–694.
[7]S. R. Bank, M. A. Wistey, L. L. Goddard, H. B. Yuen, V. Lordi, and J. S. Harris, Jr., IEEE J. Quantum Electron. **40**, 656 (2004).
[8]S. R. Bank, M. A. Wistey, H. B. Yuen, L. L. Goddard, H. Bae, and J. S. Harris, Jr., J. Vac. Sci. Technol. B **23**, 1337 (2005).
[9]J. S. Harris, in *Physics and Applications of Dilute Nitrides*, edited by I. A. Buyanova and W. M. Chen (Taylor and Francis, New York, 2004), Vol. 21, pp. 395–433.
[10]J. S. Harris, Jr., H. B. Yuen, S. R. Bank, M. A. Wistey, V. Lordi, T. Gugov, H. Bae, and L. L. Goddard, in *Dilute Nitride Seminconductors*, edited by M. Henini (Elsevier, Oxford, 2005), pp. 1–92.
[11]K. Volz, V. Gambin, W. Ha, M. A. Wistey, H. Yuen, S. Bank, and J. S. Harris, J. Cryst. Growth **251**, 360 (2003).
[12]S. R. Bank, M. A. Wistey, H. B. Yuen, V. Lordi, V. F. Gambin, and J. S. Harris, Jr., J. Vac. Sci. Technol. B **23**, 1320 (2005).
[13]D. R. Myers, S. R. Kurtz, K. Emery, C. Whitaker, and T. Townsend, in Conference Record of the Twenty-eighth IEEE Photovoltaic Specialists Conference, Anchorage, Alaska, 15–22 September (2000), p. 1202.
[14]M. J. Romero, S. Ostapenko, M. M. Al-Jassim, I. Tarasov, and P. Sheldon, in 13th Workshop on Crystalline Silicon Solar Cell Materials and Processes: Extended Abstracts and Papers from the Workshop held 10–13 August, Vail, CO (2003), p. 235.
[15]B. G. Yacobi and D. B. Holt, J. Appl. Phys. **59**, R1 (1986).
[16]S. Kurtz, J. F. Geisz, D. J. Friedman, J. M. Olson, A. Duda, N. H. Karam, R. R. King, J. H. Ermer, and D. E. Joslin, in Conference Record of the Twenty-eighth IEEE Photovoltaic Specialists Conference, Anchorage, Alaska, 15–22 September (2000), p. 1210.
[17]S. Kurtz, J. F. Geisz, D. J. Friedman, A. J. Ptak, R. R. King, D. C. Law, and N. H. Karam, in Conference Record of the Thirty-first IEEE Photovoltaic Specialists Conference, Lake Buena Vista, Florida, 3–7 January (2005), p. 707–710.
[18]S. R. Kurtz, A. A. Allerman, C. H. Seager, R. M. Sieg, and E. D. Jones, Appl. Phys. Lett. **77**, 400 (2000).
[19]D. J. Friedman, J. M. Olson, S. Ward, T. Moriarty, K. Emery, S. Kurtz, A. Duda, R. R. King, H. L. Cotal, D. R. Lillington, J. H. Ermer, and N. H. Karam, in Conference Record of the Twenty-eighth IEEE Photovoltaic Specialists Conference, Anchorage, Alaska, 15–22 September (2000), p. 965–967.
[20]A. J. Ptak, D. J. Friedman, and S. Kurtz, J. Vac. Sci. Technol. B (to be published).
[21]P. Fewster, *X-Ray Scattering From Semiconductors*, 2nd ed. (Imperial College Press, London, 2003).

Downloaded 13 Jul 2007 to 171.66.249.62. Redistribution subject to AIP license or copyright, see http://jap.aip.org/jap/copyright.jsp